Check for updates

Buoyancy and Brownian motion of plastics in aqueous media: predictions and implications for density separation and aerosol internal mixing state

Alison Bain [iD]

The low densities of many plastics compared to those of aqueous salt solutions has made density separation, relying on buoyancy overcoming Brownian motion, a convenient technique to separate nano- and microplastics from environmental matrices. Nanoplastics (smaller than about 1 μm) and microplastics (smaller than 5 mm) also exist in aqueous media in the environment, where they too will be buoyant or undergo Brownian motion and diffusion depending on their size and density. Recent evidence of plastics being introduced to the aerosol phase through bubble bursting and wave action indicates that sea-spray aerosol may contain nanoplastics, but the mixing state of this plastic in aerosol droplets is unknown. Here, the Peclet number (Pe) is used to first estimate the smallest plastics that can be separated from environmental matrices *via* density separation. These calculations predict that using a dense brine solution such as $ZnCl_2$, plastics down into the nanoplastic size range can be separated. Pe is then calculated for polyethylene terephthalate (PET), polystyrene (PS) and polyethylene (PE) plastics as a function of relative humidity for NaCl, $(NH_4)_2SO_4$ and citric acid aerosol. Calculated Pe values suggest that plastics smaller than 750 nm will always be dominated by Brownian motion regardless of relative humidity while larger plastics may become buoyant at low relative humidities.

Introduction

Since the large scale production of plastics began in the 1950s, huge amounts of plastic waste have been introduced to our environment.[1] This plastic does not biodegrade, but slowly, over time, breaks up into smaller and smaller pieces through mechanical action, action by some microbes and UV irradiation.[2] Typically, pieces smaller than 5 mm are classified as microplastics. The classification of nanoplastics is still under debate and upper size cutoffs of 0.1–1 μm have been used to define nanoplastics.[3–6] Environmental aging not only alters the size of plastic pieces but may also increase their density, and alter their colour and surface chemistry.[2,7,8] Nano- and microplastics are ubiquitous in our environment and have been found in surface waters,[9,10] soils,[11,12] ice cores,[13] urban center atmospheric fallout,[14,15] and remote terrestrial environments.[16–19]

Much of the work investigating environmental plastics has focused on the microplastic size range even though nanoplastics are expected to greatly outnumber

School of Chemistry, University of Bristol, Cantock's Close, Bristol, UK.
E-mail: alison.bain@bristol.ac.uk

microplastics.[20] This is largely due to limitations of processes to separate plastics from environmental matrices and characterization techniques.[21–24] A wide range of plastics have been found in the environment including polyethylene terephthalate (PET), polystyrene (PS), polypropylene (PP), polyethylene (PE) acrylic and nylon.[25] Density separation, historically used in the recycling process to separate plastics of different densities,[26] has proven to be a highly effective method for the separation of microplastics from environmental matrices. This technique involves introducing a sample containing microplastics to a brine solution. Over time, a film of microplastics forms on the top of the brine solution, which can then be collected, while other biological materials fall to the bottom. Such separations have been employed using a number of salt solutions, including $ZnCl_2$, NaCl and NaI.[4,16,27,28] Although NaCl brine is less dense than either $ZnCl_2$ or NaI, the cost and environmental impact of $ZnCl_2$ and NaI limit their use.[11,24]

Nano- and microplastics also exist in aqueous systems in the environment, where size and density impact their internal mixing state. Plastics in the ocean will remain buoyant or begin to settle through the water column based on their density and size.[10] Nano- and microplastics undergoing Brownian motion, and diffusing through the

This journal is © The Royal Society of Chemistry 2022

Environ. Sci.: Nano, 2022, **9**, 4249–4254 | **4249**

seawater, can be circulated back to the surface during bubble bursting events akin to other sediments.[29] Additionally, plastics have recently been found to be introduced to the aerosol phase through the bubble bursting mechanism, resulting in mixed-phase, sea-spray with plastic inclusions.[21,28,30]

Atmospheric plastics are commonly collected as filter samples,[16,19,21,28,31] as fallout in jars,[32] and have been collected from the surface of freshly fallen snow[18] as well as from car surfaces following dust storms.[33] After characterization these methods are capable of determining if plastics are present, but their mixing state cannot be obtained. Aerosol, and atmospheric nano- and microplastics may exist in external mixtures or become internally mixed in the same droplet. Aerosol droplets containing multiple phases can in turn take on a number of morphologies including homogeneous mixtures, core–shell and partially engulfed.[34] Direct observation of atmospheric microplastics to characterize the aerosol mixing state has not yet been achieved and laboratory characterization of mixed phase aerosol is difficult to achieve without influencing the system.[35,36] Predictions for the mixing state of nanoplastics in internally mixed droplets would be advantageous to design experiments probing the impacts these plastics have on our current understanding of aerosol processes and chemistry.

In the following sections, first the minimum size of nano- and microplastics, having a broad range of densities, that can be separated from various brine solutions is estimated using the Peclet number (Pe). Pe is then calculated as a function of relative humidity (RH) for NaCl, $(NH_4)_2SO_4$ and citric acid aerosol in order to predict the internal mixing state of mixed-phase aerosol-plastic systems. Finally, the significance of these results to the separation of nano- and microplastics from environmental matrices and to our understanding of plastic-containing atmospheric aerosol is discussed.

Density separation

On the macroscopic scale, we expect an object more dense than a fluid to sink and an object less dense than a fluid to float. However, as the size of the object decreases, the rate of diffusion can overcome the rate of advection. Density separation relies on buoyancy dominating over Brownian motion and can be assessed using Pe:[37–39]

$$Pe = \frac{2\pi\Delta\rho g r^4}{3k_B T} \tag{1}$$

where $\Delta\rho = \rho_{aq} - \rho_{plastic}$, the difference in density between the aqueous solution and the plastic, g is the gravitational constant (9.81 m s^{-2}), r is the particle radius, k_B is Boltzmann's constant (1.38 × 10^{-23} J K^{-1}) and T is the absolute temperature (298 K used here as plastic densities are known at room temperature). Pe greater than one indicates gravitation forces dominate (and Brownian motion can be ignored) while Pe between zero and one indicates

Brownian motion will dominate (and gravitation can be ignored).[38–40] The Pe number will be negative if the plastic is more dense than the solution. In this case the plastic will not be buoyant at any size. A Pe equal to one then indicates the transition between these regimes. For the case of nano- and microplastics in aqueous solutions, a Pe number less than one will indicate the plastic will freely diffuse through the aqueous phase, and may eventually settle to the bottom over a timescale determined by the plastic size and aerosol viscosity, while plastics with Pe greater than one will be buoyant and remain on the surface.

Using eqn (1) the minimum size of plastic that can be sampled using density separation can be estimated. Fig. 1 shows Pe greater or less than one calculated for all combinations of typical plastic densities, 0.9–2.3 g cm^{-3},[5] and solutions ranging in density from 0.997 g cm^{-3} (water) to 2.1 g cm^{-3} (saturated ZnCl$_2$) at 298 K. The gray shaded region indicates Pe less than one where Brownian motion dominates and plastic pieces are expected to diffuse through the brine and the white region indicates Pe greater than one where plastic pieces are expected to be buoyant and float on a brine solution. Horizontal lines indicate the density differences for NaCl (dashed, ρ = 1.2 g cm^{-3}) and ZnCl$_2$ (solid, ρ = 2.1 g cm^{-3}) brines with PET (red, ρ = 1.4 g cm^{-3}), PS (green, ρ = 1.075 g cm^{-3}) and PE (blue, ρ = 0.950 g cm^{-3}) plastics.

In Fig. 1, for the case of NaCl brine (dashed lines), only PE and PS in the microplastic size range (i.e. >1 μm) can be collected from the surface of a brine following density separation. For PET in NaCl brine, $\Delta\rho$ is a negative number, resulting in a negative Pe. Thus, Brownian motion and settling will dominate at all PET particle sizes. In the case of ZnCl$_2$, all plastic types in the larger nanoplastic and microplastic range could be separated, with smaller sizes being able to be separated for the lowest density plastics. As the most common microplastic characterization techniques, μ-Raman and μ-IR, have limits of detection of about 5 and 20
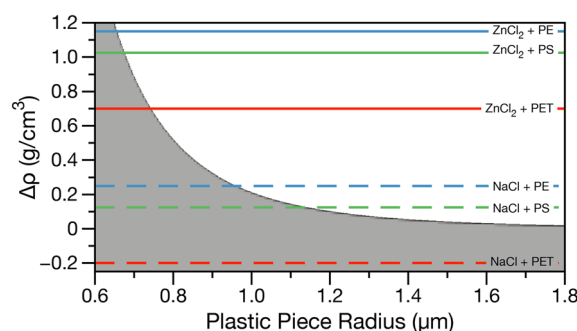

Fig. 1 Pe calculated at all possible $\Delta\rho$ for the range of aqueous densities between water and saturated ZnCl$_2$ (0.997–2.1 g cm^{-3}) and plastics (0.9–2.3 g cm^{-3}) at 298 K. Pe less than one (gray region) indicating Brownian motion dominates and greater than one (white region) indicating buoyancy dominates. Solid horizontal lines show separation of PE (blue), PS (green) and PET (red) plastics in saturated ZnCl$_2$ brine and dashed lines show separation of PE (blue), PS (green) and PET (red) plastics in saturated NaCl brine.

μm respectively,[21,24] density separation with sufficiently dense brine will not be the limiting factor in characterizing nano- and microplastic size distributions. However, if the density of the plastics in an environmental matrix is unknown or expected to include PET, NaCl brine separation will not be adequate as higher density plastics cannot be recovered.

Density separation implications for aerosol internal mixing state

Recent evidence of plastics being introduced to the aerosol phase with sea-spray[28,30] introduces the question: how do these plastics mix in aerosol droplets? In a laboratory study, Bronk *et al.* characterize plastic beads embedded in a droplet.[41] They trap 30 μm diameter saturated saltwater droplets containing an average of 163 polymer beads of diameter 460 nm in an electrodynamic balance. Using the stated density of the seawater (1.2 g cm^{-3}) and the beads (1.05 g cm^{-3}) at 298 K the Pe for this system is 0.002 and implies that Brownian motion will dominate over buoyancy.

Indeed, Bronk *et al.* observe gradual settling of the beads in the saturated seawater droplet using photon correlation spectroscopy.[41] Also utilizing an electrodynamic balance, Haddrell *et al.* characterize glycerol droplets ($\rho = 1.261$ g cm^{-3}) with 400 and 800 nm diameter PS beads.[42] Assuming a density of 1.075 g cm^{-3} for PS and a temperature of 298 K, the Pe for these systems are 0.001 and 0.02 respectively, again suggesting Brownian motion will dominate. Angular Mie scattering patterns collected from these droplets show irregularities in the intensity but not the angle of the peaks, consistent with solid inclusions.[42]

In the aerosol phase, the concentration of solute, and consequently the droplet density, will change as it undergoes hygroscopic growth or dries in order to stay in equilibrium with the relative humidity (RH) of the surrounding air. This means there is potential for a humidity dependence on the internal mixing state of plastics in aqueous aerosol.

Pe was calculated at 298 K for the example cases of aqueous NaCl, $(NH_4)_2SO_4$ and citric acid aerosol with PET, PS and PE plastics. These solutes are commonly used to approximate sea-spray, anthropogenic and organic aerosol in
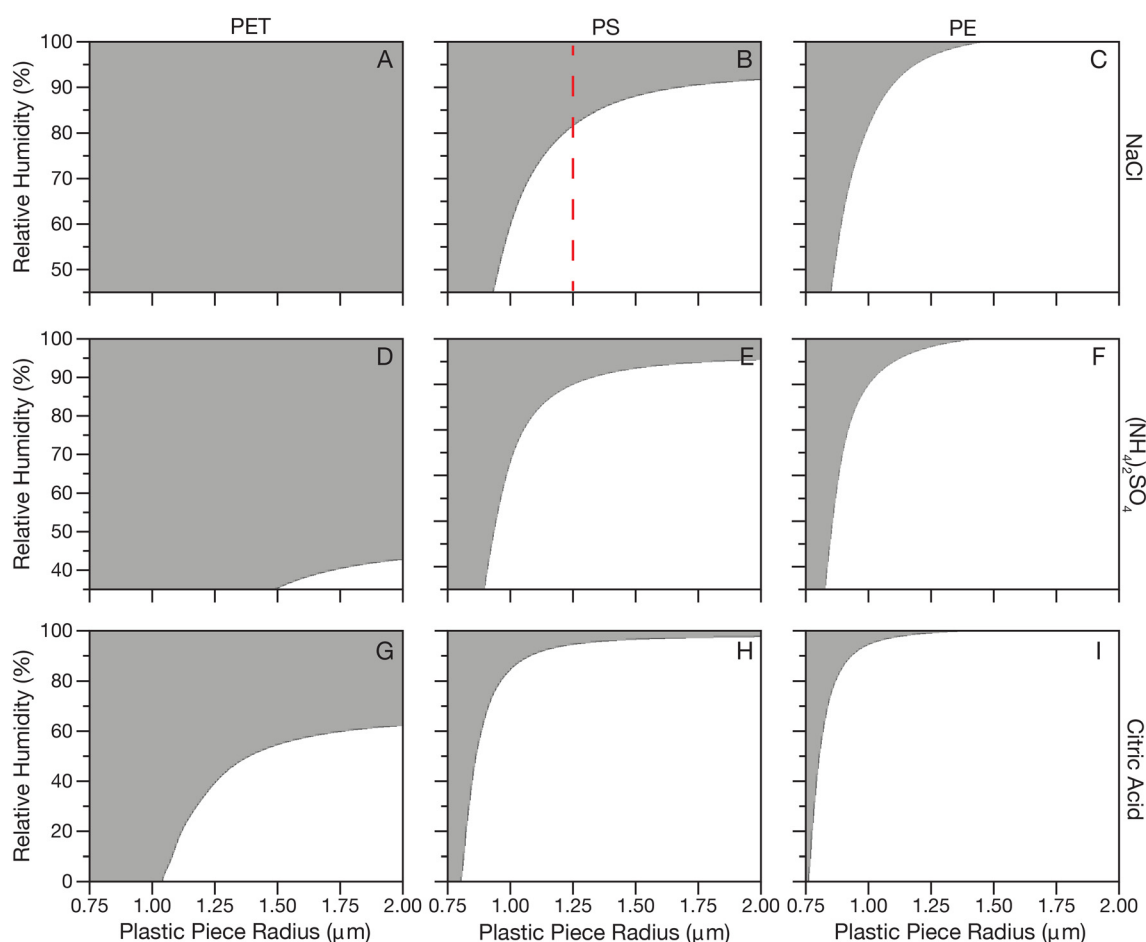

Fig. 2 Pe less than 1 (shaded regions) indicating Brownian motion dominates and greater than 1 (white regions) indicating buoyancy dominates for NaCl (top row, panels A–C), $(NH_4)_2SO_4$ (middle row, panels D–F) and citric acid (bottom row, panels G–I) with PET (left column, panels A, D and G), PS (middle column, panels B, E and H) and PE (right column, panels C, F and I) at RHs where these systems could exist in the aqueous phase. The red dashed vertical line in panel B indicates the predicted internal mixing state for a 1.25 μm radius PS particle in NaCl aerosol as a function of RH.

This journal is © The Royal Society of Chemistry 2022

Environ. Sci.: Nano, 2022, **9**, 4249–4254 | **4251**

laboratory experiments.[43] Sea-spray aerosol will contain both plastics and NaCl while atmospheric plastics from other sources such as waste incineration may be mixed with $(NH_4)_2SO_4$.[28,31] Citric acid was also included to serve as an example of aqueous organic aerosol. Unlike NaCl and $(NH_4)_2SO_4$, citric acid and other aqueous organic aerosol do not effloresce but retain some of their water content down to 0% RH, yielding a large range in density. PET, PS and PE plastics were chosen since they span a wide range of densities and are commonly found in atmospheric fallout and in remote locations where atmospheric transport followed by deposition is thought to be the source.[14,16,19]

The water activity (a_w) as a function of solute mass fraction for NaCl, $(NH_4)_2SO_4$ and citric acid systems were calculated at 298 K using AIOMFAC.[44,45] For droplets larger than about 100 nm where surface curvature can be neglected, water activity and RH are related through $a_w = RH/100$.[46] Density as a function of RH was then determined for NaCl and $(NH_4)_2SO_4$ aerosol by fitting the mass fraction and density data from the CRC handbook[47] to a second order polynomial. This fit was extrapolated to supersaturated conditions until the efflorescence point. For citric acid, the density parameterization from Lienhard et al. was used.[48]

Pe was calculated up to a maximum plastic radius of 2 μm. Size distributions of freshly emitted sea-spray aerosol are commonly measured under dry conditions and can span orders of magnitude, typically with a film drop mode centered around a diameter of about 1 μm.[29] Under high RH conditions, the diameter of hygroscopic aerosol can double. Still, only the largest sea-spray droplets would be able to contain this upper limit in plastic radius.

Fig. 2 shows calculated Pe for NaCl, $(NH_4)_2SO_4$ and citric acid systems at a range of RHs (efflorescence RH-100% RH for salts and 0–100% RH for citric acid) and particle sizes for PET, PS and PE plastics. Panel A shows that PET in NaCl aerosol at any RH is predicted to be dominated by Brownian motion and diffuse through the droplet due to the high density of PET compared to even a supersaturated NaCl solution. In panel B, moving to the less dense PS, larger pieces of plastic are predicted to partition to the surface at low RHs, but at the highest RHs and smallest sizes, plastics will mix in the droplet bulk. For example, the dashed red line in panel B shows that for plastic radius 1.75 μm, under humid conditions above about 80% RH the density of an NaCl droplet would be such that Brownian motion of the plastic would dominate but if the RH of the surrounding air decreased leading to evaporation of water from the droplet, the resulting increase in density suggests the plastic would become buoyant. In panel C for PE a similar trend is observed, but pushed to smaller plastic sizes due to the lower density of PE. In panels D–F, for $(NH_4)_2SO_4$, a similar trend is observed as for NaCl, but the lower efflorescence RH of $(NH_4)2SO_4$ leads to a larger range in Δρ pushing the transition from buoyant to diffusing plastics to smaller plastic sizes. Finally, in panels G–I for citric acid, which has the largest range in density with RH, the transition from buoyant to diffusing plastics is again pushed to higher RHs and smaller plastic sizes.

Environmental significance and conclusions

Density separation of nano- and microplastics is well established and actively used in the microplastics field to separate plastics from environmental matrices. Calculated Pe suggests that this technique is useful in the separation of sizes less than 1 μm, below the limit of detection of common characterization techniques for typical environmental plastics and achievable densities of salt solutions. Density separation, however, is not appropriate for samples containing dense plastics such as PET or if quantification of nanoplastics is required.

Aerosol droplets in the atmosphere range in diameter from only a few nanometers in the accumulation mode to several microns in the coarse mode,[49] while cloud droplets can reach diameters of tens of microns.[50] This size range overlaps with the size range of microplastics (<5 mm) and nanoplastics (<1 μm). Atmospheric microplastics and larger sized nanoplastics will occupy most of the volume a mixed phase particle. Smaller nanoplastics, however, have the potential to become internally mixed in droplets. Pe calculated for atmospheric aerosol and common environmental plastics shows that, depending on nanoplastic type, size and the RH of the surrounding air, nanoplastics may sit on the droplet surface or be free to diffuse through the droplet bulk. Sufficiently large and/or dense inclusions may settle while holding droplets stationary for laboratory analysis,[35,41] but under atmospheric conditions where droplets rotate a few times a second[51] could remain in the droplet interior. Aerosol viscosity, which can vary by orders of magnitude,[52,53] in addition to the plastic piece size, will determine the rate of diffusion of nanoplastics through the aerosol.[41] Of note, regardless of the aqueous system and plastic type, plastics of radius less than 750 nm are predicted to be dominated by Brownian motion and diffuse through the aerosol at all RHs. Recent quantification of nanoplastics less than 200 nm in diameter from remote Alpine snow samples suggests that sub 750 nm radius nanoplastics are indeed transported through the atmosphere.[54] Although difficult to characterize, nanoplastics in the environment are expected to greatly outnumber microplastics since larger pieces are continuously being broken up into more, smaller fragments.[3,20]

It must be noted that the calculated Pe for nanoplastics in aerosol represent ideal conditions and in the context of ambient aerosol more complex situations may arise. First, nano- and microplastics found in the environment are only sometimes spherical, and more often are identified as fragments or fibers. Here it was assumed these morphologies can be approximated as ellipsoids, taking the longest radius as r in eqn (1). This assumption may slightly shift the transition in Pe for ambient plastics. Second, plastic can

4252 | Environ. Sci.: Nano, 2022, **9**, 4249–4254

This journal is © The Royal Society of Chemistry 2022

become electrostatically charged and may form clusters. Using the settling time of the beads and the viscosity of seawater, Bronk *et al.* retrieved a radius for their beads almost three times larger than expected. They suggest confinement inside a droplet increases the probability of forming small clusters.[41] Cluster formation will alter the apparent radius and density of the plastic. Third, the temperature in the atmosphere varies greatly with altitude, and ambient aerosol droplets can exist in a supercooled state.[55] Pe, and thus the internal mixing state, will be affected by a change in temperature and the resulting change in densities of both the aqueous phase and plastic inclusions.

Experimental work is needed to characterize the mixing state of nanoplastic inclusions in aerosol droplets and test these internal mixing state predictions. Experiments should investigate how different plastic morphologies affect its internal mixing state in aerosol, if plastic inclusions form clusters inside droplets and if cluster formation is affected by droplet size or changing RH conditions. Characterizing solid inclusions in aerosol droplets without influencing them proves difficult[35,36] and new techniques are needed meet this challenge. A better understanding of the mixing state of plastic inclusions in ambient aerosol is necessary to predict how these plastics will alter our current understanding of aerosol properties such as diffusion of water in and out of the droplets,[7] chemistry occurring on the surface of the plastic or due to the leaching of chemical species from the plastic into the aqueous phase,[56–58] and their ability to act as ice nuclei.[59]

Conflicts of interest

There are no conflicts to declare.

Acknowledgements

References

1   R. Geyer, J. R. Jambeck and K. L. Law, *Sci. Adv.*, 2017, **3**, 25–29.
2   Y. K. Song, S. H. Hong, M. Jang, G. M. Han, S. W. Jung and W. Shim, *J. Environ. Sci. Technol.*, 2017, **51**, 4368–4376.
3   J. Gigault, A. ter Halle, M. Baudrimont, P. Y. Pascal, F. Gauffre, T. L. Phi, H. El Hadri, B. Grassl and S. Reynaud, *Environ. Pollut.*, 2018, **235**, 1030–1034.
4   Y. Picó and D. Barceló, *ACS Omega*, 2019, **4**, 6709–6719.
5   V. Hidalgo-Ruz, L. Gutow, R. C. Thompson and M. Thiel, *Environ. Sci. Technol.*, 2012, **46**, 3060–3075.
6   J. Gigault, H. El Hadri, B. Nguyen, B. Grassl, L. Rowenczyk, N. Tufenkji, S. Feng and M. Wiesner, *Nat. Nanotechnol.*, 2021, **16**, 501–507.
7   A. Bain and T. C. Preston, *Environ. Sci. Technol.*, 2021, **55**, 11775–11783.
8   X. Liu, Q. Deng, Y. Zheng, D. Wang and B. J. Ni, *Water Res.*, 2022, **221**, 118780.
9   Y. K. Song, S. H. Hong, M. Jang, G. M. Han, M. Rani, J. Lee and W. J. Shim, *Mar. Pollut. Bull.*, 2015, **93**, 202–209.
10 L. M. Rios Mendoza and M. Balcer, *TrAC, Trends Anal. Chem.*, 2019, **113**, 402–408.
11 J. N. Mo, M. G. J. L. Der and C. Laforsch, *Environ. Sci. Technol.*, 2020, **54**, 2078–2090.
12 J. Wang, X. Liu, Y. Li, T. Powell, X. Wang, G. Wang and P. Zhang, *Sci. Total Environ.*, 2019, **691**, 848–857.
13 A. Kelly, D. Lannuzel, T. Rodemann, K. M. Meiners and H. J. Auman, *Mar. Pollut. Bull.*, 2020, **154**, 111130.
14 L. Cai, J. Wang, J. Peng, Z. Tan, Z. Zhan, X. Tan and Q. Chen, *Environ. Sci. Pollut. Res.*, 2017, **24**, 24928–24935.
15 M. Klein and E. K. Fischer, *Sci. Total Environ.*, 2019, **685**, 96–103.
16 S. Allen, D. Allen, V. R. Phoenix, G. Le Roux, P. Durántez Jiménez, A. Simonneau, S. Binet and D. Galop, *Nat. Geosci.*, 2019, **12**, 339–344.
17 J. Brahney, M. Hallerud, E. Heim, M. Hahnenberger and S. Sukumaran, *Science*, 2020, **368**, 1257–1260.
18 M. Bergmann, S. Mützel, S. Primpke, M. B. Tekman, J. Trachsel and G. Gerdts, *Sci. Adv.*, 2019, **5**, 1–11.
19 S. Allen, D. Allen, F. Baladima, V. R. Phoenix, J. L. Thomas, G. Le Roux and J. E. Sonke, *Nat. Commun.*, 2021, **12**, 7242.
20 A. Bianco and M. Passananti, *Sustainability*, 2020, **12**, 7327.
21 M. Trainic, J. M. Flores, I. Pinkas, M. L. Pedrotti, F. Lombard, G. Bourdin, G. Gorsky, E. Boss, Y. Rudich, A. Vardi and I. Koren, *Commun. Earth Environ.*, 2020, **1**, 1–9.
22 J. Gigault, B. Pedrono, B. Maxit and A. Ter Halle, *Environ. Sci.: Nano*, 2016, **3**, 346–350.
23 M. Gniadek and A. Dabrowska, *Mar. Pollut. Bull.*, 2019, **148**, 210–216.
24 Y. Zhang, S. Kang, S. Allen, D. Allen, T. Gao and M. Sillanpää, *Earth-Sci. Rev.*, 2020, **203**, 103118.
25 H. Yang, Y. He, Y. Yan, M. Junaid and J. Wang, *Nanomaterials*, 2021, **11**, 1–20.
26 S. Serranti and G. Bonifazi, *UUe of Recycled Plastics in Eco-efficient Concrete*, Elsevier Ltd, 2019, pp. 9–37.
27 B. Nguyen, D. Claveau-Mallet, L. M. Hernandez, E. G. Xu, J. M. Farner and N. Tufenkji, *Acc. Chem. Res.*, 2019, **52**, 858–866.
28 S. Allen, D. Allen, K. Moss, G. Le Roux, V. R. Phoenix and J. E. Sonke, *PLoS One*, 2020, **15**, 1–14.
29 X. Wang, G. B. Deane, K. A. Moore, O. S. Ryder, M. D. Stokes, C. M. Beall, D. B. Collins, M. V. Santander, S. M. Burrows, C. M. Sultana and K. A. Prather, *Proc. Natl. Acad. Sci. U. S. A.*, 2017, **114**, 6978–6983.
30 M. Masry, S. Rossignol, B. T. Roussel, D. Bourgogne, P.-O. Bussière, B. R'mili and P. Wong-Wah-Chung, *Environ. Pollut.*, 2021, **280**, 116949.
31 K. Liu, X. Wang, T. Fang, P. Xu, L. Zhu and D. Li, *Sci. Total Environ.*, 2019, **675**, 462–471.
32 R. Dris, J. Gasperi, M. Saad, C. Mirande and B. Tassin, *Mar. Pollut. Bull.*, 2016, **104**, 290–293.
33 S. Abbasi, M. Rezaei, F. Ahmadi and A. Turner, *Chemosphere*, 2022, **292**, 133456.

This journal is © The Royal Society of Chemistry 2022

Environ. Sci.: Nano, 2022, **9**, 4249–4254 | **4253**

34 B. J. Dennis-Smither, K. L. Hanford, N. O. A. Kwamena, R. E. H. Miles and J. P. Reid, *J. Phys. Chem. A*, 2012, **116**, 6159–6168.

35 U. K. Krieger and A. A. Zardini, *Faraday Discuss.*, 2007, **137**, 377–388.

36 A. M. Laurain and J. P. Reid, *J. Phys. Chem. A*, 2009, **113**, 7039–7047.

37 A. K. A. Ahmed, C. Sun, L. Hua, Z. Zhang, Y. Zhang, T. Marhaba and W. Zhang, *Environ. Eng. Sci.*, 2018, **35**, 720–727.

38 Y. Li, X. Wang, W. Fu, X. Xia, C. Liu, J. Min, W. Zhang and J. C. Crittenden, *Water Res.*, 2019, **161**, 486–495.

39 N. M. Kovalchuk and V. M. Starov, *Adv. Colloid Interface Sci.*, 2012, **179-182**, 99–106.

40 A. S. Dukhin, S. S. Dukhin and P. J. Goetz, *Adv. Colloid Interface Sci.*, 2007, **134-135**, 35–71.

41 B. V. Bronk, S. Arnold and M. J. Smith, *Opt. Lett.*, 1993, **18**, 93–95.

42 A. Haddrell, G. Rovelli, D. Lewis, T. Church and J. Reid, *Aerosol Sci. Technol.*, 2019, **53**, 1334–1351.

43 A. Bain, A. Rafferty and T. C. Preston, *Geophys. Res. Lett.*, 2019, **46**, 10636–10645.

44 A. Zuend, C. Marcolli, B. P. Luo and T. Peter, *Atmos. Chem. Phys.*, 2008, **8**, 4559–4593.

45 Aerosol Inorganic-Organic mixtures Functional groups Activity Coefficients. https://aiomfac.lab.mcgill.ca, last accessed: 09/02/2022.

46 S. Bezantakos, L. Huang, K. Barmpounis, S. T. Martin and G. Biskos, *J. Aerosol Sci.*, 2016, **101**, 1–9.

47 "*CRC Handbook of Chemistry and Physics*" *Concentrative Properties of Aqueous Solutions*, ed. J. R. Rumble, CRC Press/ Taylor & Francis, Boca Raton, FL., 102nd edn, 2021.

48 D. M. Lienhard, D. L. Bones, A. Zuend, U. K. Krieger, J. P. Reid and T. Peter, *J. Phys. Chem. A*, 2012, **116**, 9954–9968.

49 P. K. Quinn, D. B. Collins, V. H. Grassian, K. A. Prather and T. S. Bates, *Chem. Rev.*, 2015, **115**, 4383–4399.

50 W. K. Tao, J. P. Chen, Z. Li, C. Wang and C. Zhang, *Rev. Geophys.*, 2012, **50**, RG2001.

51 P. C. Arroyo, G. David, P. A. Alpert and E. A. Parmentier, *Science*, 2022, **376**, 293–296.

52 Y. C. Song, A. E. Haddrell, B. R. Bzdek, J. P. Reid, T. Bannan, D. O. Topping, C. Percival and C. Cai, *J. Phys. Chem. A*, 2016, **120**, 8123–8137.

53 B. R. Bzdek, L. Collard, J. E. Sprittles, A. J. Hudson and J. P. Reid, *J. Chem. Phys.*, 2016, **145**, 054502.

54 D. Materić, A. Kasper-Giebl, D. Kau, M. Anten, M. Greilinger, E. Ludewig, E. Van Sebille, T. Röckmann and R. Holzinger, *Environ. Sci. Technol.*, 2020, **54**, 2353–2359.

55 D. A. Knopf, P. A. Alpert and B. Wang, *ACS Earth Space Chem.*, 2018, **2**, 168–202.

56 S. He, M. Jia, Y. Xiang, B. Song, W. Xiong, J. Cao, H. Peng, Y. Yang, W. Wang, Z. Yang and G. Zeng, *J. Hazard. Mater.*, 2022, **424**, 127286.

57 X. Li, H. Zhao, B. Qu and Y. Tian, *Chemosphere*, 2022, **291**, 132815.

58 K. Zhu, H. Jia, W. Jiang, Y. Sun, C. Zhang, Z. Liu, T. Wang, X. Guo and L. Zhu, *Environ. Sci. Technol.*, 2022, **56**, 779–789.

59 M. Ganguly and P. A. Ariya, *ACS Earth Space Chem.*, 2019, **3**, 1729–1739.

4254 | *Environ. Sci.: Nano*, 2022, **9**, 4249–4254

This journal is © The Royal Society of Chemistry 2022